Rate Dependent Progressive Composite Damage Modeling using MAT162 in LS-DYNA®

Bazle Z. (Gama) Haque[1,2], and John W. Gillespie Jr.[1,2,3,4]
[1] *University of Delaware Center for Composite Materials (UD-CCM)*
[2] *Department of Mechanical Engineering*
[3] *Department of Materials Science & Engineering*
[4] *Department of Civil & Environmental Engineering*
University of Delaware, Newark, DE 19716

Abstract

Performing experiments in numerical space and predicting accurate results are the main research focus of many computational mechanicians. These goals may in general sound challenging, however, makes perfect sense in cases where experiments are not possible, e.g., landing on Mars, sea waves impacting marine structures, crash landing of space shuttle, etc. Composite damage modeling plays a vital role in designing composite structures for damage tolerance, energy dissipating crash, impact, ballistic, and blast applications. A progressive composite damage model MAT162 is developed by Materials Sciences Corporation and further modified by the authors and implemented in explicit finite element analysis code LS-DYNA. A total of thirty-four material properties and parameters are required to define such a material model. Besides the ASTM standard test methods for determining the elastic and strength properties, the authors have developed a low velocity impact methodology in determining the rate insensitive model parameters. Recently, model validations with depth of penetration and ballistic experiments have been performed to determine the rate sensitive model parameters. These validated model parameters are used to predict composite damage and resistance behavior of composite structures made from plain-weave plain weave S-2 glass/SC15 composites under quasi-static, low velocity impact and crush, ballistic, and blast loading conditions. Analysis procedure and results of these numerical experiments will be presented.

Introduction

Prediction of reasonable composite damage and retention of properties after quasi-static (QS), fatigue, low velocity impact (LVI), high velocity ballistic impact (HVBI), and blast loading is of great interest to many civil, government, and aerospace industries. In order to be able to solve such problems, one needs a progressive composite damage model (pCDM) that can predict the initiation and evolution of different composite damage modes [1-4] using well established failure theories [5-10] and continuum damage mechanics [11-13] models. In order to solve dynamic problems, one must develop such a pCDM and implement the same in an explicit finite element code e.g., LS-DYNA, AutoDyn, ABAQUS, etc. In solving static and fatigue problems, an implicit finite element code is necessary, e.g., ANSYS, ABAQUS, NASTRAN, etc.

Such a pCDM for uni-directional (UD) and plain-weave (PW) fabric composites has been developed by Materials Sciences Corporation (MSC) [14] and University of Delaware Center for

Composite Materials (UD-CCM) [15], which is also known as MAT162, and is implemented in LS-DYNA. The objective of this paper is to provide an overview of research performed by the authors, and the ongoing research elucidating the capabilities of the progressive composite damage model MAT162 under a wide range of loading conditions.

Rate Dependent Progressive Composite Damage Modeling using MAT162

General Description of MAT162

MAT162 is the state-of-the-art in three dimensional progressive damage modeling of UD and PW composites using solid elements and explicit analysis in LS-DYNA. This material model was developed on the foundation of earlier orthotropic composite models, i.e., MAT02 and MAT59. The detailed formulation of these material models can be found in the LS-DYNA Keyword manual [14]. The MAT162 input properties and parameters for PW S-2 Glass/SC15 composites is presented in Table 1 [16, 17]. In addition to nine elastic constants (EA, EB, EC, PRBA, PRCA, PRCB, GAB, GBC, & GCA), this material model uses ten strength parameters (SAT, SAC, SBT, SBC, SCT, SFS, SFC, SAB, SBC, SCA) to define the yield point after linear-elastic deformation, two material parameters (SFFC, PHIC) to define residual strength after compression and Mohr-Coulomb type friction factor, two modeling variables (S_DELM, OMGMX) to define stress concentration at the delamination front and maximum admissible modulus reduction, and three erosion parameters (E_LIMT, E_CRSH, EEXPN) for eroding elements to allow penetration or to create free surfaces. Based on Hashin's theory [6], five quadratic failure criteria for UD composites and seven failure criteria for PW composites are defined to model different composite damage modes, e.g., matrix crack, delamination, fiber tension-shear, fiber compression, fiber shear, and composite crush (Table 2). The most important aspect of MAT162 is the capability of modeling post-damage softening behavior of composites using continuum damage mechanics while degrading the material properties following a connectivity matrix of different damage modes. This method of progressive damage is achieved using an exponential damage function with the softening parameter "m" for four different damage modes, e.g., m1 for fiber damage in material direction 1 or A, m2 for fiber damage in material direction 2 or B, m3 for fiber crush and punch shear, and m4 for matrix crack and delamination. In addition, the rate effects on strength properties are modeled with four rate parameters, CERATEs. The values of the damage parameters m can vary between a large negative and a large positive number, and depending on a specific material behavior, four discrete values need to be chosen to run any numerical simulation. Since a large number of simulations need to be conducted to identify a suitable set of m values that defines a material behavior, it is usually suggested that these parametric computations be conducted on a unit single element [18, 19]. UD-CCM has developed a series of single element numerical experiments to perform these parametric simulations which can be found at the official MAT162 website [15].

Progressive Damage Modeling in MAT162

Following the suggestion by Matzenmiller et al. [11], the post-damage softening behavior of a composite is modeled by an exponential function with four parameters, i.e., m1 for fiber damage in material direction 1 or ‘A’, m2 for fiber damage in material direction 2 or ‘B’, m3 for fiber

crush and punch shear damage, and m4 for matrix crack and delamination damage. A maximum admissible modulus reduction parameter (OMGMX) is used to define the fraction of modulus reduction, the value of which is less than one, e.g., OMGMX = 0.999. Reduction in modulus is defined by an exponential function given by:

$$\varpi = 1 - e^{\frac{1}{m}\left(1-\left(\frac{\varepsilon}{\varepsilon_y}\right)^m\right)} \qquad [1]$$

Table 1. MAT162 Properties and Rate-Dependent Parameters for PW S-2 Glass/SC15 [16,17]

MID	RO, kg/m^3	EA, GPa	EB, GPa	EC, GPa	PRBA	PRCA	PRCB
162	1850.00	27.50	27.50	11.80	0.11	0.18	0.18
GAB, GPa	GBC, GPa	GCA, GPa	AOPT	MACF			
2.90	2.14	2.14	2	1			
XP	YP	ZP	A1	A2	A3		
0	0	0	1	0	0		
V1	V2	V3	D1	D2	D3	BETA	
0	0	0	0	1	0	0	
SAT, MPa	SAC, MPa	SBT, MPa	SBC, MPa	SCT, MPa	SFC, MPa	SFS, MPa	SAB, MPa
600	300	600	300	50	800	250	75
SBC, MPa	SCA, MPa	SFFC	AMODEL	PHIC	E_LIMT	S_DELM	
50	50	0.3	2	10	0.2	1.20	
OMGMX	ECRSH	EEXPN	CERATE1	AM1*			
0.999	0.001	4.0	0.030	2.00			
AM2*	AM3*	AM4*	CERATE2	CERATE3	CERATE4		
2.00	0.50	0.35	0.000	0.030	0.030		

* AM1, AM2, AM3, and AM4 are LS-DYNA variables for parameters m1, m2, m3 and m4.

Table 2. Failure criterion of MAT162 progressive damage model.

UNI-DIRECTIONAL COMPOSITE		**PLAIN-WEAVE COMPOSITE**	
Damage Mode	**Criterion**	**Damage Mode**	**Criterion**
Fiber tension/shear	$\left(\frac{E_1.\langle\varepsilon_1\rangle}{X_{1,T}}\right)^2 + \frac{G_{12}^2\varepsilon_{12}^2 + G_{31}^2\varepsilon_{31}^2}{S_{FS}^2} = r_1^2$	Fill Fiber tension/shear	$\left(\frac{E_1.\langle\varepsilon_1\rangle}{X_{1,T}}\right)^2 + \left(\frac{G_{31}\varepsilon_{31}}{S_{FS}}\right)^2 = r_1^2$
Fiber compression	$\left(\frac{E_1.\langle\varepsilon_1^{'}\rangle}{X_{1,C}}\right)^2 = r_2^2 \quad \varepsilon_1^{'} = -\varepsilon_1 - \frac{\langle -E_2\varepsilon_2 - E_3\varepsilon_3\rangle}{2E_1}$,	Fill Fiber compression	$\left(\frac{E_1.\langle\varepsilon_1^{'}\rangle}{X_{1,C}}\right)^2 = r_2^2 \quad \varepsilon_1^{'} = -\varepsilon_1 - \langle -\varepsilon_3\rangle\frac{E_3}{E_1}$
Fiber crush	$\left(\frac{E_3\langle -\varepsilon_3\rangle}{S_{FC}}\right)^2 = r_3^2$	Warp Fiber tension/shear	$\left(\frac{E_2.\langle\varepsilon_2\rangle}{X_{2,T}}\right)^2 + \left(\frac{G_{23}\varepsilon_{23}}{S_{FS}}\right)^2 = r_3^2$
Transverse compression	$\left(\frac{E_2\langle -\varepsilon_2\rangle}{X_{2,C}}\right)^2 = r_4^2$	Warp Fiber compression	$\left(\frac{E_2.\langle\varepsilon_2^{'}\rangle}{X_{2,C}}\right)^2 = r_4^2 \quad \varepsilon_2^{'} = -\varepsilon_2 - \langle -\varepsilon_3\rangle\frac{E_3}{E_2}$,
Perpendicular matrix crack	$\left(\frac{E_2.\langle\varepsilon_2\rangle}{X_{2,T}}\right)^2 + \left(\frac{G_{23}.\varepsilon_{23}}{S_{23}+S_{SRB}}\right)^2 + \left(\frac{G_{12}.\varepsilon_{12}}{S_{12}+S_{SRB}}\right)^2 = r_5^2$	Fiber crush	$\left(\frac{E_3 < -\varepsilon_3 >}{S_{FC}}\right)^2 = r_5^2$
Parallel matrix (Delamination)	$S^2\left\{\left(\frac{E_3.\langle\varepsilon_3\rangle}{X_{3,T}}\right)^2 + \left(\frac{G_{23}.\varepsilon_{23}}{S_{23}+S_{SRC}}\right)^2 + \left(\frac{G_{31}.\varepsilon_{31}}{S_{31}+S_{SRC}}\right)^2\right\} = r_6^2$	Perpendicular matrix crack	$\left(\frac{G_{12}\varepsilon_{12}}{S_{12}}\right)^2 = r_6^2$
$* S_{SRB} = E_2\tan(\phi)\langle -\varepsilon_2\rangle$ $S_{SRC} = E_3\tan(\phi)\langle -\varepsilon_3\rangle$		Parallel matrix (Delamination)	$S^2\left\{\left(\frac{E_3.\langle\varepsilon_3\rangle}{S_{3,T}}\right)^2 + \left(\frac{G_{23}.\varepsilon_{23}}{S_{23}+S_{SRC}}\right)^2 + \left(\frac{G_{31}.\varepsilon_{31}}{S_{31}+S_{SRC}}\right)^2\right\} = r_7^2$

where, ϖ is the modulus reduction parameter, m is the softening parameter, and ε_y is the yield strain. The post-yield modulus E and stress σ can then be expressed as:

$$E = (1-\varpi)E_0 = E_0\, e^{\frac{1}{m}\left(1-\left(\frac{\varepsilon}{\varepsilon_y}\right)^m\right)} \quad [2]$$

$$\sigma = E\varepsilon = E_0\, \varepsilon\, e^{\frac{1}{m}\left(1-\left(\frac{\varepsilon}{\varepsilon_y}\right)^m\right)} \quad [3]$$

where, E_0 is the input modulus. Dimensionless stress up to and beyond the yield point and can then be expressed as:

$$\frac{\sigma}{\sigma_y} = \frac{\varepsilon}{\varepsilon_y} \quad \text{for} \quad \frac{\varepsilon}{\varepsilon_y} \le 1 \quad [4a]$$

$$\frac{\sigma}{\sigma_i} = \frac{\varepsilon}{\varepsilon_y} e^{\frac{1}{m}\left(1-\left(\frac{\varepsilon}{\varepsilon_y}\right)^m\right)} \quad \text{for} \quad \frac{\varepsilon}{\varepsilon_y} > 1 \quad [4b]$$

Figure 1 shows the dimensionless stress as a function of dimensionless strain defined by Eq. [4] for different m values. For a very high positive value of *m*, e.g. *m* = 100, the post-yield stress-strain behavior can be considered as brittle failure. For a near zero value of *m*, e.g. *m* = 0.01, the post-yield behaviour is almost perfectly plastic. Values of *m* in the range 0 < *m* < 100 show different degrees of post-yield softening behavior.

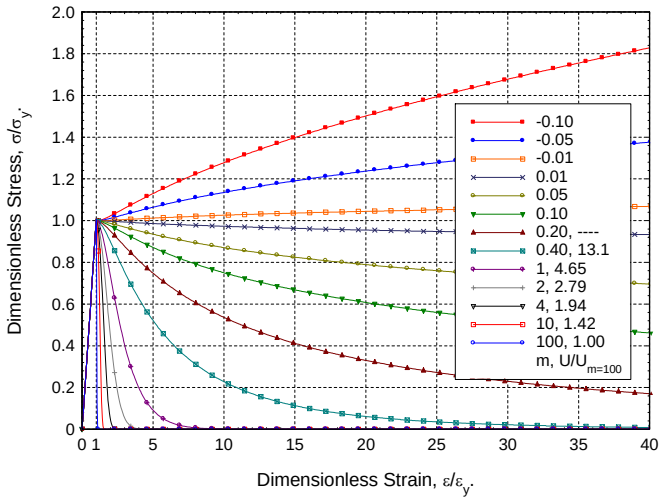

Figure 1. Post-Yield Damage Model Implemented in MAT162.

The post damage hardening behavior of a material can be modeled using a negative value of *m*; however, one must be careful with this parameter since the strain energy will keep increasing until the element is eroded/deleted. Eroding an element with high strain energy is a well-known reason for instabilities in explicit computation, and should be avoided if possible. Figure 1 also shows the dimensionless strain energy for different *m* values, where strain energy for *m* = 100 is considered as the baseline elastic-brittle failure behavior. As the *m* value is reduced from 100 to 0.40, the strain energy is increased by a factor of 13.1 as compared to the elastic-brittle material behavior. This formulation of post-damage softening is applied to define tension, compression

and shear in all three principal material co-ordinates. The user must conduct a series of single element experiments under uni-axial stress and strain loading conditions and under combined loading [18, 19].

The damage function φ describes the fraction of stiffness degradation for each damage mode, and is expressed as:

$$\varphi = 1 - e^{\frac{1}{m}(1-r^m)} \qquad [5]$$

where *m* is a softening parameter of a material, and *r* is the damage threshold which has the initial value of unity before the damage initiated, and are updated due to damage accumulation in the associated damage modes. Since different failure modes (φ_j) affect a specific material degradation, MAT 162 defines the maximum damage variable as the modulus reduction parameter (ϖ_i):

$$\varpi_i = \max\left\{\varphi_j q_{ij}\right\} \qquad i = 1,2,...,6, \qquad \begin{matrix} j = 1,2,...,6 & UD \\ j = 1,2,...,7 & PW \end{matrix} \qquad [6]$$

where q_{ij} relates the individual damage variables φ_j to the various damage modes provided by the damage functions of the UD and PW fabric models.

$$[q_{uni}] = \begin{bmatrix} 1 & 1 & 1 & 0 & 0 & 0 \\ 0 & 0 & 1 & 1 & 1 & 0 \\ 0 & 0 & 1 & 0 & 0 & 1 \\ 1 & 1 & 1 & 1 & 1 & 0 \\ 0 & 0 & 1 & 1 & 1 & 1 \\ 1 & 1 & 1 & 0 & 0 & 1 \end{bmatrix}, \quad [q_{fabric}] = \begin{bmatrix} 1 & 0 & 1 & 0 & 1 & 0 & 0 \\ 0 & 1 & 0 & 1 & 1 & 0 & 0 \\ 0 & 0 & 0 & 0 & 1 & 0 & 1 \\ 1 & 1 & 1 & 1 & 1 & 1 & 0 \\ 0 & 1 & 0 & 1 & 1 & 0 & 1 \\ 1 & 0 & 1 & 0 & 1 & 0 & 1 \end{bmatrix} \qquad [7]$$

Based on equation [7], a new compliance matrix ($[\mathbf{S}]$) is obtained to model progressive damage as expressed in Equation [8].

$$[\mathbf{S}] = \begin{bmatrix} \frac{1}{(1-\varpi_1)E_1} & \frac{-\nu_{21}}{E_2} & \frac{-\nu_{31}}{E_3} & 0 & 0 & 0 \\ \frac{-\nu_{12}}{E_1} & \frac{1}{(1-\varpi_2)E_2} & \frac{-\nu_{32}}{E_3} & 0 & 0 & 0 \\ \frac{-\nu_{13}}{E_1} & \frac{-\nu_{23}}{E_2} & \frac{1}{(1-\varpi_3)E_3} & 0 & 0 & 0 \\ 0 & 0 & 0 & \frac{1}{(1-\varpi_4)G_{12}} & 0 & 0 \\ 0 & 0 & 0 & 0 & \frac{1}{(1-\varpi_5)G_{23}} & 0 \\ 0 & 0 & 0 & 0 & 0 & \frac{1}{(1-\varpi_6)G_{31}} \end{bmatrix} \quad [8]$$

Examples of Composite Damage Modeling using MAT162

Prediction of Damage under Quasi-Static Loading

In our previous paper, we have presented several quasi-static loading cases to predict the evolution of damage and related non-linear load-displacement plots. Among them includes, (i) Quasi-Static Open Hole Compression, (ii) Quasi-Static Open Hole Tension, (iii) and Quasi-Static Four Point Bend Open Hole Flexure [20]. In this paper we will present the quasi-static damage behavior of 3D orthogonal weave fabric (OWF) composites.

Progressive Damage Modeling of 3D OWF Composites

A 2×2 Unit Cell Model (UCM) of 3D S-2 Glass/SC15 OWF composite is developed as shown in Figure 2. Unit cell models of the 3D OWF composite are composed of (i) warp (X) and fill (Y) tows through the thickness, (ii) a S-shaped Z-tow, and (iii) the interstitial resin gaps as shown in Figure 2. The dimension of the 2×2 UCM is, 9.236 mm×10.16 mm×5.39 mm. Tows in the UCM of 3D OWF composite are modeled using MAT162 uni-directional (UD) material model with UD S-2 Glass/SC15 material properties, and SC15 resin is modeled using a visco-plastic material model to reflect strain rate effects under later ballistic loading.

MAT162 UD model is adopted for S-2 Glass/SC15 modeling. Fundamental coupon tests of uni-directional (UD) S-2 Glass/SC15 composites were done according to ASTM standards. Both tension and compression along fiber and transverse directions were performed. In-plane and out-of-plane shear properties are measured as well. Fiber volume fraction of UD composite used for these tests is about 60%. Table 3 shows the summary of experimental results with numerical parameters for uni-directional S-2 Glass/SC15 composites. Quasi-static and high strain rate testing have been conducted to determine the visco-plastic behavior of SC15 resin. The experimental data is used as the material input for MAT24, and the unit single element analysis is used to predict the visco-plastic behavior of SC15 resin (Fig. 3).

Axial tension and compression behavior of the 2x2 unit cell of the 3D OWF composite is presented in Fig. 4. The solid blue curve shows the non-linear response of the 2x2 UCM of 3D OWF composite, and the plots with solid symbols show the equivalent behavior of MAT162 PW model with different modeling parameters. It is obvious that a unique set of PW MAT162 parameter does not exist to model the behavior of 3D OWF composites, which is true because the PW damage definitions cannot be used to model the 3D damage behavior. Fig. 5a shows the through-thickness tensile behavior and Fig. 5b shows the interlaminar shear. Clearly, the non-linear deformation and damage mechanisms of 3D OWF composites cannot be modeled with MAT162 PW approximation and new material module need to be developed to address these issues.

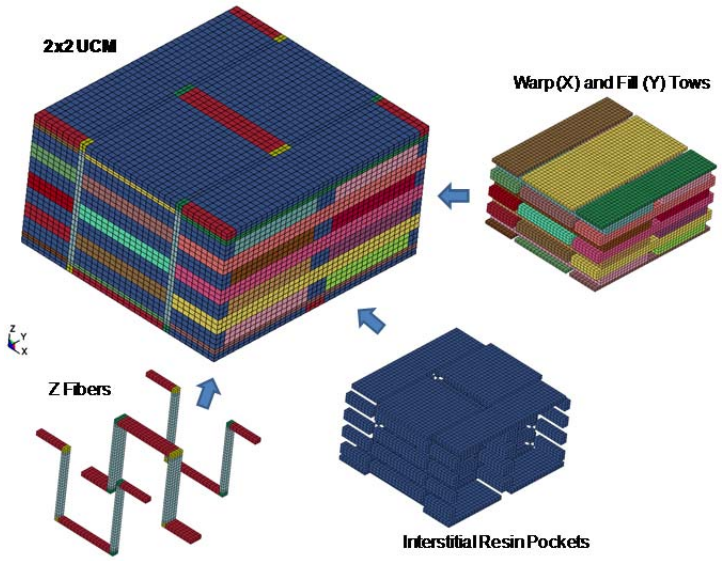

Figure 2. 2×2 Unit Cell Model (UCM) of 3D S-2 Glass/SC15 OWF Composites.

Table 3. Material properties of UD S-2 Glass/SC15 Composites for MAT162 input.

MID	**Density, kg/m^3**	**E_1, GPa**	**E_2, GPa**	**E_3, GPa**	**ν_{21}**	**ν_{31}**	**ν_{32}**
162	1850.00	64.00	11.80	11.80	0.0535	0.0535	0.449
G_{12}, GPa	**G_{23}, GPa**	**G_{31}, GPa**					
4.30	3.70	4.30					
$X_{1,T}$, MPa	**$X_{1,C}$, MPa**	**$X_{2,T}$, MPa**	**$X_{2,C}$, MPa**	**$X_{3,T}$, MPa**	**S_{FC}, MPa**	**S_{FS}, MPa**	**S_{12}, MPa**
1380.00	770.00	47.00	137.00	47.00	850.00	250.00	76.00
S_{23}, MPa	**S_{31}, MPa**	**SFFC**	**PHIC**	**E_LIMIT**	**S_DELM**		
38.00	76.00	0.100	10	0.200	1.200		
OMGMX	**ECRSH**	**EEXPN**	**C_{rate1}**	**AM1**			
0.999	0.005	2.000	0.030	100.00			
AM2	**AM3**	**AM4**	**C_{rate2}**	**C_{rate3}**	**C_{rate4}**		
10.0	1.00	0.10	0.000	0.030	0.030		

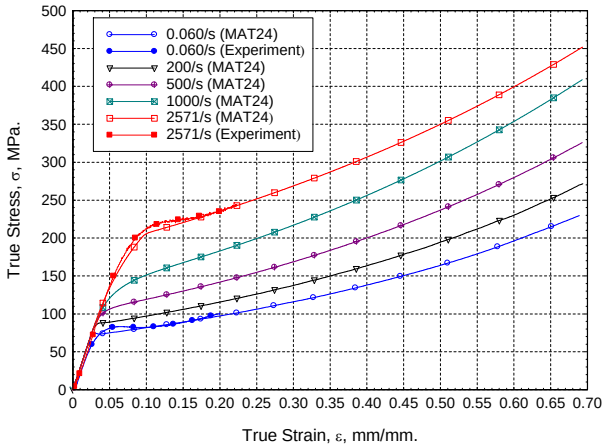

Figure 3. Visco-Plastic Behavior of SC15 Resin.

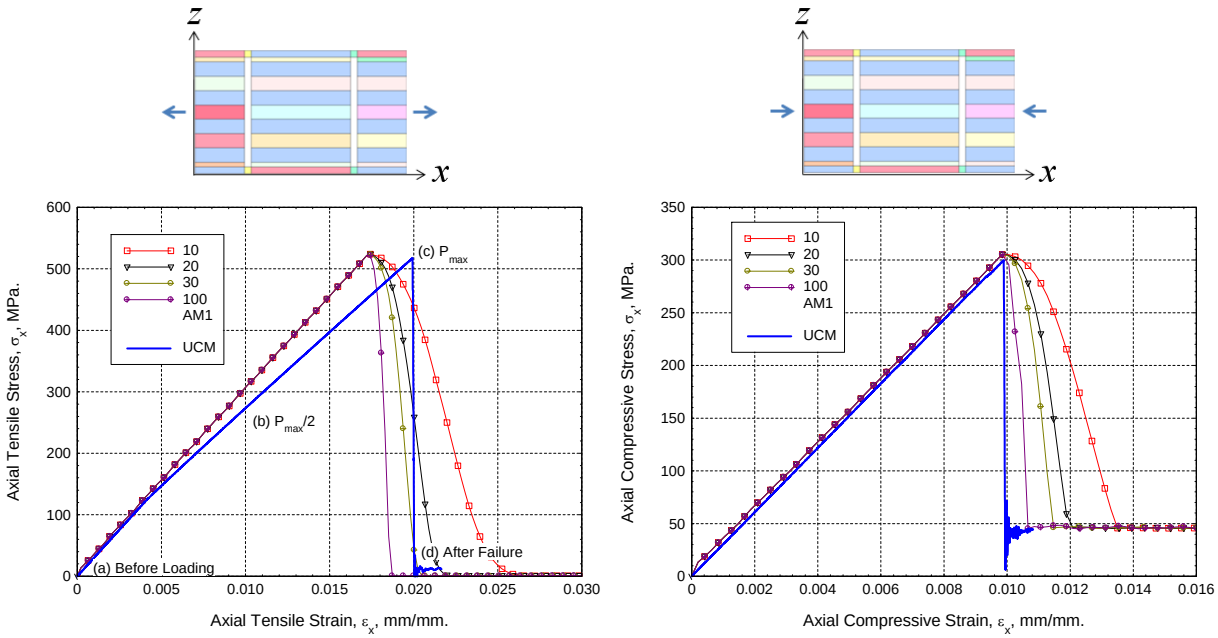

(a) X-Tension (b) X-Compression

Figure 4. In-Plane Tension and Compression Behavior of 3D OWF Composite Unit Cells.

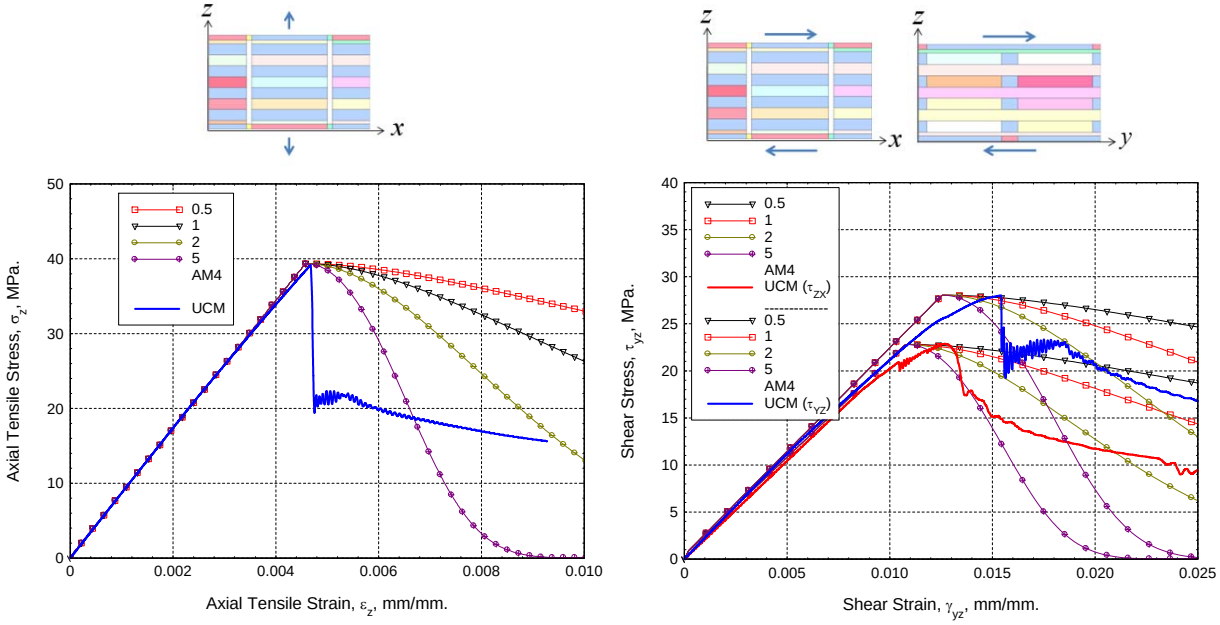

(a) Z-Tension (b) XZ & YZ Interlaminar Shear

Figure 5. Through-Thickness Tension and Interlaminar Shear Behavior of 3D OWF Composite Unit Cells.

Prediction of Damage under Low Velocity Impact Loading

Low velocity impact (LVI) loading can be successfully modeled using explicit analysis. Compression after Impact (CAI) is a popular LVI test method in aerospace industries. We will present the prediction of LVI damage and dynamics of the projectile-composite plate pair, and the prediction of CAI damage for different impact cases. In both cases, LVI experiments are performed on composite plates of dimensions, L×W×H = 152.4-mm × 101.6-mm × 5.28-mm. A 25.4-mm wide clamped boundary condition on all four edges is assumed. The composite laminate is made from eight layers of PW S-2 Glass/SC15 laminas with a stacking sequence of $[\pm 90/\pm 45]_{2S}$. The projectile used in LVI experiment is a cylinder of diameter 12.7-mm with a hemispherical cap.

Prediction of Low Velocity Impact Damage and Projectile Dynamics

Figure 6a shows the impact damage and dynamic deformation of the composite plate, and Figure 6b shows the impact force as a function of time for three impact velocities. It took about 5ms for the hemispherical projectile to rebound from the composite laminate after impact. A reasonable match between the experiment and prediction is observed. The CAI simulation is presented next.

Prediction of Compression After Impact Damage

In order to model the strength retention of the composite laminates after low velocity impact, in-plane axial displacements have been applied to the edges of the composite specimen to mimic a realistic CAI experiment. Appropriate boundary conditions are also applied. Knowing the duration of LVI event to be 5ms, another 5ms time is allowed for the model to spring back. At time T = 10ms, axial compressive displacement is applied to the model for another 20ms. Figure

7a shows the LVI damage and spring back of the plate at T = 10ms, and the CAI damage at T = 30ms. Figure 7b shows the LVI response in the time range 0ms < T < 10ms, and the CAI response in the time range 10ms < T < 30ms. The progression of damage and kink-band formation is captured in the numerical simulation. Three different ultimate loads under axial compression are predicted for three different LVI cases. These results will be validated with experiments and will remain as future works.

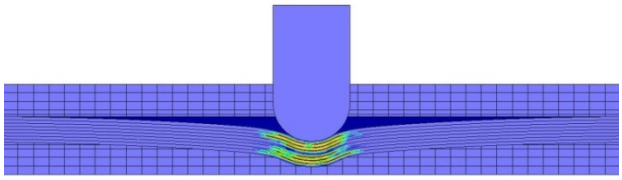

(a) LVI Damage

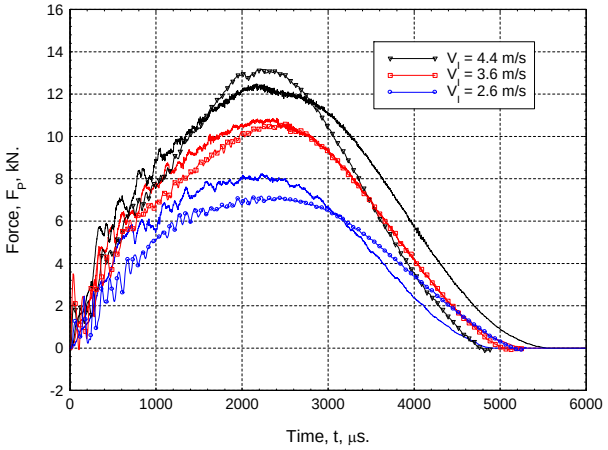

(b) LVI Impact Force - Time. Symbols - Experimental Data, Line - Predictions

Figure 6. Prediction of Low Velocity Impact Experiments using MAT162.

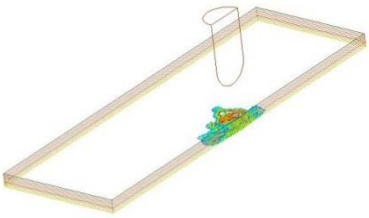

LVI Damage, T = 10ms

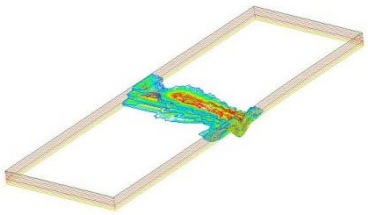

CAI Damage, T = 30ms

(a) LVI & CAI Damage

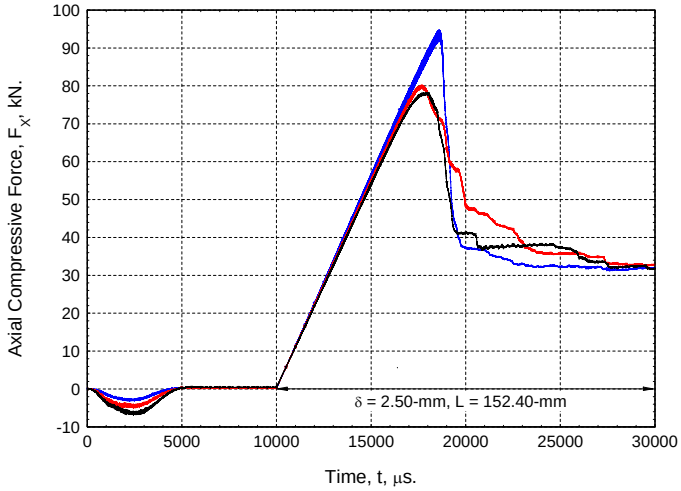

BLUE - 2.6 m/s
RED - 3.6 m/s
BLACK - 4.4 m/s

(b) LVI and CAI Response

Figure 7. Prediction of Compression After Impact Experiments using MAT162.

Prediction of Damage under High Velocity Ballistic Impact

Penetration mechanics of thick-section composites is an active research area of the authors. Results of high velocity impact damage have been presented in a recent conference [16], and will also be presented in this conference as a companion paper by Manzella et al. (2010) [20].

Prediction of Ballistic Damage under High Velocity Impact

The example presented here is taken from our paper presented in Ref. [16]. A finite element model of the ballistic experiments has been developed (Figure 8). The model is validated with ballistic experiments, and the rate dependent modeling parameters has been determined and is presented in Table 1.

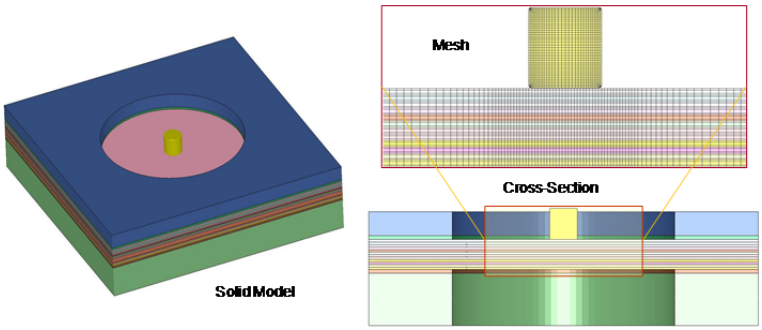

Figure 8. 3D Finite Element Model of Ballistic Impact on Thick-Section Composite.

Time, μs	V_I = 360 m/s, V_I / V_{BL} = 0.98	V_I = 400 m/s, V_I / V_{BL} = 1.09
20	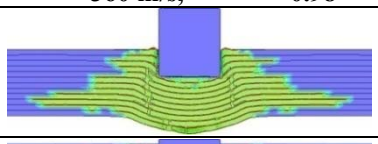	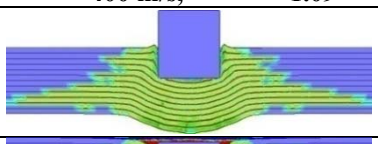
60	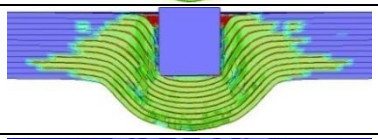	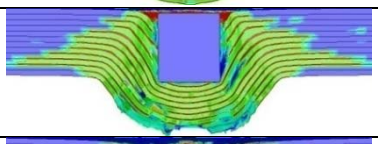
100	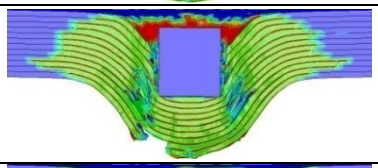	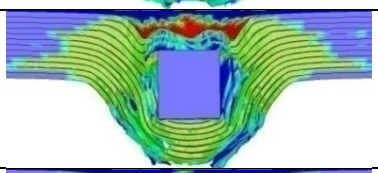
200	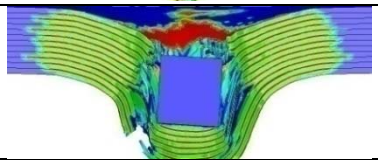	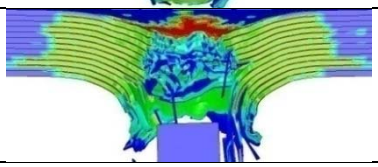
End of Experiment with Spring Back		

Figure 9. Prediction of Ballistic Damage below and above Ballistic Limit.

Figure 9 shows the prediction of ballistic damage of a 13.2-mm thick composite plate (22 Layers of PW S-2 Glass/SC15) subjected to the impact of a 12.7-mm right circular cylinder projectile below and above the ballistic limit velocity V_{BL} (or V_{50}) of the target. This validated model has been used to predict the ballistic impact damage of composites for which ballistic experiments have not been performed, and such an example is presented in the next section.

Ballistic Performance of Damaged Composites

An obvious questions comes into mind, can MAT162 predict ballistic limit of impact damaged composites? In order to answer this question, two projectiles are impacted on the baseline laminate described in the earlier example. The first projectile creates damage under non penetrating impact velocities, i.e., 50 m/s & 300 m/s; and the second projectile impact at a much higher velocity than the ballistic limit, i.e., 500 m/s. Fig. 10 shows the ballistic damage befor and after the second impact, while Fig. 11 shows the projectile instantaneous velocities for both the projectiles.

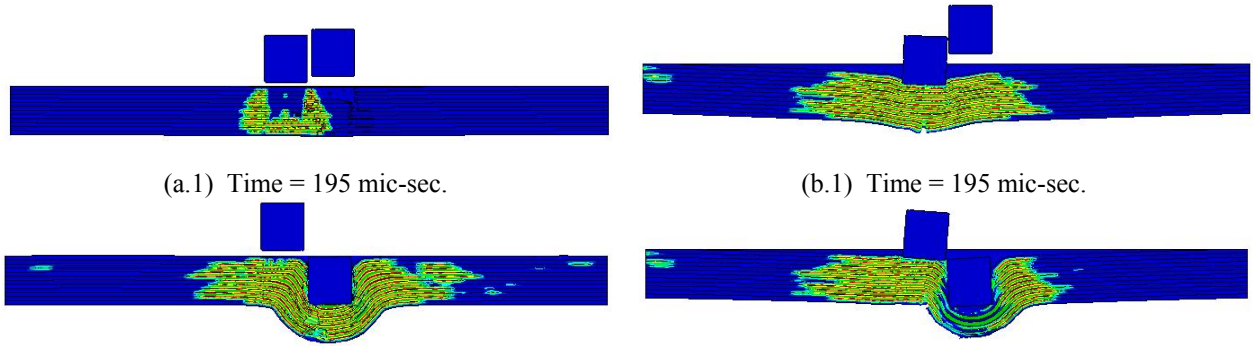

(a.1) Time = 195 mic-sec. (b.1) Time = 195 mic-sec.

(a.2) Time = 245 mic-sec. V_1 = 50 m/s, V_2 = 500 m/s

(b.2) Time = 245 mic-sec. V_1 = 300 m/s, V_2 = 500 m/s.

Figure 10: Ballistic Impact on Damaged Composite Laminate.

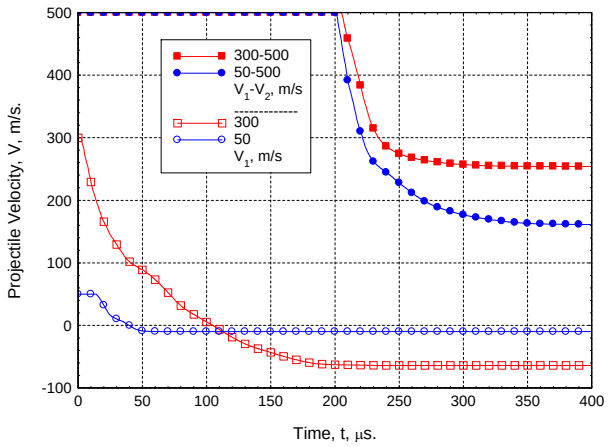

Figure 11. Projectile Velocities for two Projectiles at two Different Impact Scenarios.

When impacted with V_1 = 50 m/s impact velocity, the projectile rebounded with a velocity equal to -9.9 m/s. The second projectile (V_2 = 500 m/s) completely penetrated the composite plate and the residual velocity is found to be 161 m/s. For the first impact at V_1 = 300 m/s, significant damage is created and the projectile rebounded with an rebound velocity equal to -64 m/s. The

second projectile (V_2 = 500 m/s) completely penetrated the composite plate and the residual velocity is found to be 254 m/s. This increase in residual velocity is indicative of less penetration resistance offered by a damage composite laminate. Future work will investigate the compression after ballistic impact and ballistic resistance of damaged composite laminates.

Prediction of Damage under BLAST LOADING

*Blast Modeling with CONWEP *LOAD_BLAST_ENHANCHED Function*

A 610-mm × 610-mm (2-ft x 2-ft) plate of 48.8 kg/m^2 (10 psf) areal-density is considered for analysis. FE models of an aluminum plate, an aluminum foam sandwich panel with aluminum face sheets, and a monolithic thick-section composite plate are developed. The CONWEP blast load of a 2-kg TNT equivalent spherical charge at a 610-mm (2-ft) standoff distance (SoD) is applied on all three models (on top and above the plate). Dynamics of deformation and damage of composite plate is under investigation, and has been presented in 11th LS-DYNA Conference.

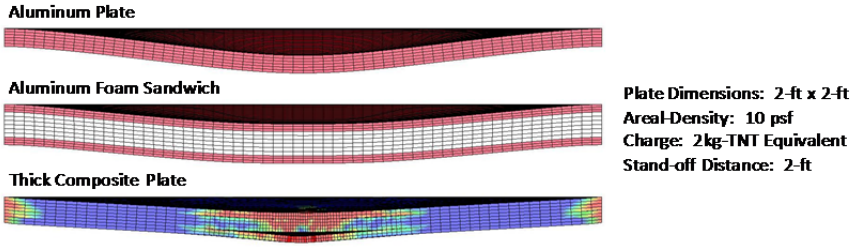

Figure 12. Prediction of High Velocity Perforation of Thin Laminates using MAT162.

Blast on Composites: Particle Dynamics Approach

Modeling the buried mine interaction is a challenging task and is usually handled by Arbitrary Lagrange Euler (ALE) coupling. The soil elements deform like a fluid and transfers momentum to the structure. This approach of solution does not allow the modeling of sand or rocks embedded in a soil. We approach this problem with the particle dynamics approach. In this approach, the soil is modeled as finite size particles of different size, shape, and material, with statistically distributed properties. The research is in its early stage, where cubes, rectangular prisms, cylinders, and spheres are considered as the basic shapes. Few 3D solid elements (1 to 8) are used to model each particles, and a finite element particle generator is developed to generate a huge array of different shapes and sizes of particles based on a random number generator and several section criterion for range of percentage of different particles, range of particle size, and an completely random geometric location. The output of the particle generator is fed into a numerical shaker for packing before the particles are ready for blast applications. The application of BLAST load on these particles is considered both by CONWEP blast function, and calculating the initial velocity of the particles by dividing the CONWEP impulse by the mass of each particles. Further theoretical and computational studies are under development.

BLAST loading on 30x30x5 = 4500 sphere particles of diameter 2.54-mm (0.100-inch) on a 610-mm × 610-mm (24-in x 24-in) four layer 3D woven fabric composite plate is presented in Figure 11. A hemi-spherical surface blast loading of 500gm TNT at a SoD = 152.4-mm (6-in) is applied on the first layer of the particles using LS-DYNA blast function *LOAD_BLAST_ENHANCED. A second set of same BLAST load is applied on the composite plate. The effect of blast loading on particles, their dynamics of interaction with the composite

plate, and the transverse matrix damage of the composite predicted by LS-DYNA 971 V.4.2 shows that the particles impact the composite plate, transfers the momentum and damages the plate, and bounces back from the composite plate.

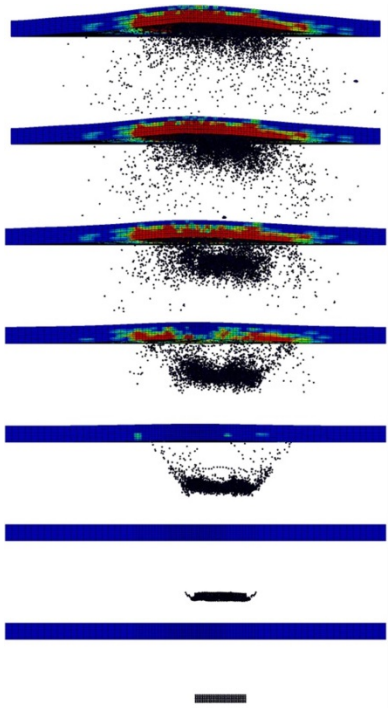

Figure 13. Modeling Surface Blast and Particle Blast on Composites using LS-DYNA MAT162 and *LOAD_BLAST_ENHANCED

Summary

Progressive composite damage modeling (pCDM) using MAT162 is presented for several QS, LVI, HVBI, and blast loading conditions. It has been shown that explicit analysis can be used to mimic QS experiments in some cases, however, for QS loading scenarios where wave speed is low, and for fatigue loading conditions, an implicit formulation of MAT162 is necessary and remains as a future work. HVBI simulations were used to validate ballistic models while determining the rate dependent properties from parametric simulations. Validated ballistic model is then used to solve ballistic and blast problems for which experimental data is not available. MAT162 is the state-of-the-art tool for progressive composite damage modeling and can further be developed to add material non-linearity, implicit formulation, and models for 2D/3D woven fabric composites other than UD and PW composites.

ACKNOWLEDGMENT

Research was sponsored by the Army Research Laboratory and was accomplished under Cooperative Agreement Number W911NF-07-2-0026. The views and conclusions contained in this document are those of the authors and should not be interpreted as representing the official policies, either expressed or implied, of the Army Research Laboratory or the U.S. Government.

References

1. Cuntze, R.G. and Freund, A., "The Predictive Capability of Failure Mode Concept-Based Strength Criteria for Multidirectional Laminates", Composites Science and Technology 64 (2004): 343–377.
2. Laš, V., and Zemčík, R., "Progressive Damage of Unidirectional Composite Panels", Journal of Composite Materials 42 (2008): 25-44.
3. Puck, A., and Schűrmann, H., "Failure Analysis of FRP Laminates by Means of Physically Based Phenomenological Models", Composites Science and Technology 58 (1998): 1045-1067.
4. Yen, C.F., and Caiazzo, A., Innovative processing of multifunctional composite armor for ground vehicles, ARL Technical Report ARL-CR-484, 2001, US Army Research Laboratory.
5. Tsai, S. W., and Wu, E. M., "A General Theory of Strength for Anisotropic Materials", Journal of Composite Materials 5 (1971): 58-80.
6. Hashin, Z., "Failure Criteria for Unidirectional Fiber Composites", Journal of Applied Mechanics 47 (1980): 329-334.
7. Sun, C. T., Quinn, B. J., and Oplinger, D. W., Comparative Evaluation of Failure Analysis Methods for Composite Laminates, DOT/FAA/AR-95/109, 1996
8. Christensen, R. M., "Stress Based Yield/Failure Criteria for Fiber Composites", International Journal of Solids and Structures 34(5) (1997): 529-543.
9. Dávila, C. G., Camanho, P. P., and Rose, C. A., "Failure Criteria for FRP Laminates", Journal of Composite Materials 39(4) (2005): 323-345.
10. Xiao, J.R., and Gillespie Jr., J. W., "A Phenomenological Mohr–Coulomb Failure Criterion for Composite Laminates under Interlaminar Shear and Compression", Journal of Composite Materials 41(11) (2007): 1295-1309.
11. Matzenmiller, A., Lubliner, J. and Taylor, R. L., "A constitutive model for anisotropic damage in fiber-composites", Mechanics of Materials 20(4) (1995): 125–152.
12. Schuecker, C., Pettermann, H. E., A Continuum Damage Model for Fiber Reinforced Laminates Based on Ply Failure Mechanisms, Composite Structures 76 (2006): 162–173.
13. Hassan, N. M., Batra, R. C., "Modeling Damage in Polymeric Composites", Composites: Part B 39 (2008): 66–82.
14. LS-DYNA Keyword User's Manual, Livermore Software Technology Corporation. Version 971, May 2007.
15. http://www.ccm.udel.edu/Tech/MAT162/Intro.htm
16. Gama, B. A., Bogetti, T. A., and Gillespie Jr, J. W., "Impact, Damage and Penetration Modeling of Thick-Section Composites using LS-DYNA MAT162", Proceedings of the 24nd ASC Annual Technical Conference, Newark, Delaware, September 15-17, 2009.
17. Xiao, J.R., Gama, B.A., and Gillespie Jr. J.W., "Progressive Damage Delamination in Plain Weave S-2 Glass/SC-15 Composites under Quasi-Static Punch-Shear Loading", Composite Structures 78 (2007): 182-196.
18. Gama, B.A., Bogetti, T.A., and Gillespie Jr., J.W. 2009. "Progressive Damage Modeling of Plain-Weave Composites using LS-DYNA Composite Damage Model MAT162," 7th European LS-DYNA Conference, Austria, May 14-15, 2009.
19. Kang, S.-G., Gama, B.A., and Gillespie Jr. J.W., "Damage Modeling of Unidirectional and 3D Composite Unit Cells", SAMPE 2010, Seattle, Washington, May 17-20, 2010.
20. Gama, B.A, Bogetti, T.A, and Gillespie Jr., J.W., "Composite Damage Modeling Under Quasi-Static, Low Velocity Impact, Ballistic and Blast Loading Conditions", SAMPE 2010, Seattle, Washington, May 17-20, 2010.
21. Manzella, A. F., Gama, B. A., and Gillespie Jr., J. W., "Effect of Laminate Thickness on Ballistic Penetration of Thick-Section Composites", SAMPE 2010, Seattle, Washington, May 17-20, 2010.